Cytogenetic and Genome Research

Novel Insights from Clinical Practice

Cytogenet Genome Res 2020;160:321–328
DOI: 10.1159/000508820

Received: December 18, 2019
Accepted: May 4, 2020
Published online: June 13, 2020

# Disruption of *PCDH10* and *TNRC18* Genes due to a Balanced Translocation

Malú Zamariolli[a] Adriana Di-Battista[a] Mariana Moysés-Oliveira[a]
Cláudia B. de Mello[b] Marco A. de Paula Ramos[a] Thomas Liehr[c]
Maria I. Melaragno[a]

[a]Genetics Division, Department of Morphology and Genetics, Universidade Federal de São Paulo, São Paulo, Brazil; [b]Psychobiology Department, Universidade Federal de São Paulo, São Paulo, Brazil; [c]Institute of Human Genetics, Jena University Hospital, Friedrich Schiller University, Jena, Germany

**Established Facts**

- Balanced translocations may be associated with phenotypic alterations through gene disruption at the breakpoints.
- Breakpoint mapping is crucial to the genotype-phenotype correlation and can be a valuable approach to annotation of disease-associated genes.

**Novel Insights**

- We report on a balanced translocation with disruption of 2 genes: *TNRC18* and *PCDH10*.
- *PCDH10* is potentially associated with our patient's intellectual disability.
- The clinical significance of *TNRC18* is unknown, and our patient's clinical description can add new insights towards the elucidation of its function and role in disease.

**Keywords**
Balanced translocations · Chimeric gene · Next-generation sequencing · *PCDH10* · *TNRC18*

**Abstract**
Balanced chromosomal rearrangements are usually associated with a normal phenotype, although in some individuals, phenotypic alterations are observed. In these patients, molecular characterization of the breakpoints can reveal the pathogenic mechanism, providing the annotation of disease-associated loci and a better genotype-phenotype correlation. In this study, we describe a patient with a balanced reciprocal translocation between 4q27 and 7p22 associated with neurodevelopmental delay. We performed cytogenetic evaluation, next-generation sequencing of microdissected derivative chromosomes, and Sanger sequencing of the junction points to define the translocation's breakpoints at base pair resolution. We found that the *PCDH10* and *TNRC18* genes were disrupted by the breakpoints at chromosomes 4 and 7, respectively, with the formation of chimeric genes at

M.Z., A.D.-B., and M.M.-O. contributed equally to this work.

karger@karger.com
www.karger.com/cgr



Maria Isabel Melaragno
Department of Morphology and Genetics
Universidade Federal de São Paulo
Rua Botucatu, 740, CEP 04023-900, São Paulo, SP (Brazil)
melaragno.maria@unifesp.br

the junction points. Gene expression studies in the patient's peripheral blood showed reduced expression of *TNRC18*, a gene with unknown function and clinical significance. *PCDH10* plays a role in the development of the nervous system and might be involved with the patient's neurodevelopmental delay. In this study, the full molecular characterization of the junction points was shown as an efficient tool for fine breakpoint mapping in balanced translocations in order to unmask gene disruptions and investigate the potential pathogenic role of the disrupted genes.



Balanced chromosome abnormalities (BCAs) consist of structural variations that alter the position and/or orientation of a DNA segment without gain or loss of genomic material. Although most carriers of BCAs are phenotypically normal, about 6% of them present an associated disease phenotype [Warburton, 1991]. The prevalence for BCAs is about 0.2–0.5% in the general population [Ravel et al., 2006] and an approximate 5-fold increase prevalence is observed in subjects with neurodevelopmental disorders [Funderburk et al., 1977]. Different pathogenic mechanisms have been attributed as causes of the phenotypic alterations in BCAs, such as gene disruptions of dosage-sensitive genes at the breakpoints [Menten et al., 2006; Schneider et al., 2015], gene disruption followed by formation of chimeric genes expressing hybrid transcripts [Di Gregorio et al., 2013; Córdova-Fletes et al., 2015], and disruption of regulatory regions resulting in separation of cis-regulatory elements from the genes they control [Zepeda-Mendoza et al., 2018]. Precise breakpoint mapping is crucial for the genotype-phenotype correlation [Redin et al., 2017; Schluth-Bolard et al., 2019] and can be an important approach to annotation of disease-associated genes. In addition to revealing pathogenic causes, the high-resolution breakpoint determination can give insights about the potential molecular mechanisms of chromosome break and repair and provide information into "mutational signatures" [Nilsson et al., 2017]. Despite the recognition of this approach as a powerful tool in searching pathogenic genomic regions, most studies on BCAs until nowadays have used only low resolution methods, such as karyotyping and FISH. Additionally, chromosomal microarray-based genome-wide surveys are unable to further characterize balanced rearrangements. The evolution of accurate and affordable next-generation sequencing (NGS) techniques, such as whole genome sequencing (WGS), has been fundamental to elucidate breakpoints at nucleotide resolution contributing to a molecular diagnosis [Aristidou et al., 2017, 2018; Schluth-Bolard et al., 2019]. Low coverage WGS, for example, is an efficient method for the detection and characterization of balanced translocations [Liang et al., 2017], and this characterization is improved when WGS is combined with cytogenomic methods [Moysés-Oliveira et al., 2019]. A more cost-effective strategy corresponds to the sequencing of specific microdissected segments from the derivative chromosomes, targeting the genomic regions surrounding the breakpoints [Jancuskova et al., 2013]. In this study, we precisely mapped the breakpoint in a patient with a balanced translocation and abnormal phenotype. We used NGS in microdissected chromosomes followed by Sanger sequencing of the junction points in order to molecularly characterize the breakpoints at a base pair resolution. Expression assays were also performed in order to address the impact of the breakpoints on the disrupted genes. We analyzed the genomic features of the breakpoint regions, inferred the rearrangement's mechanism of formation, and investigated the effect of the gene disruptions in the patient's phenotype.

## Case Report

*Patient*

The patient was a 30-year-old woman (Fig. 1a, b), second of 3 children, of a healthy non-consanguineous couple with normal siblings. Gestation was uneventful and she was born at term by cesarean section, with 2,750 g, 46 cm, cephalic perimeter of 33 cm, and Apgar score of 9/10. Regarding developmental milestones, she presented cervical spine control and social laugh at the age of 3–4 months, sat at 7 months, walked at 14 months, spoke her first words at 24 months, and presented sphincters control at 30 months. She underwent speech therapy and psychotherapy during childhood due to anxiety and learning disability, showing good evolution with therapies, enabling her complete literacy. At the age of 10 years, she presented with menarche and hirsutism, followed by irregular menstrual cycles. She also had high myopia that was corrected at the age of 19 years. Clinical evaluation at the age of 30 years revealed facial dysmorphisms, such as flat face, discrete brachycephaly, mild facial asymmetry, discrete palpebral ptosis on the right, exotropia, tele-

**Fig. 1.** Phenotype and cytomolecular data of the patient. **a** Front and **b** lateral view. **c** Hands. **d** Partial G-banding karyotype. **e** Ideogram of the chromosomes involved in the translocation showing the chimeric genes originated by the translocation and the location of the TaqMan probes used for expression studies (T1 to T3). **f**, **g** Sanger sequencing electropherograms of der(4) (**f**) and der(7) (**g**). **h**, **i** RTqPCR levels of *TNRC18* using a probe that accesses a transcript region 5′ to the breakpoint (T2) (**h**) and a probe that accesses a transcript region 3′ to the breakpoint (T3) (**i**).

*(For figure see next page.)*

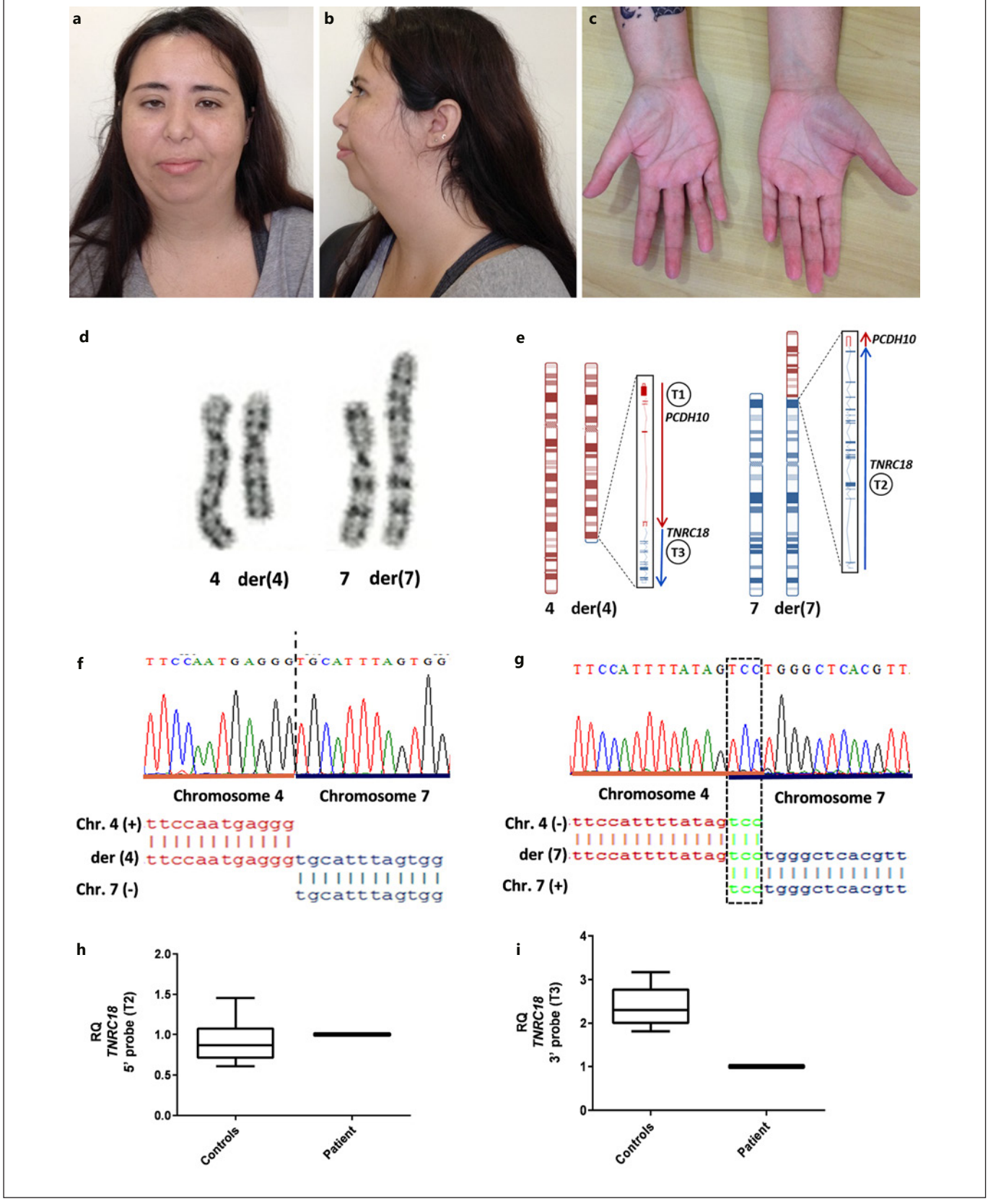


1

**Table 1.** Neuropsychological assessment results

| Cognitive domains | Percentile | Classification |
|---|---|---|
| Long-term memory | | |
| RAVLT: serial recall | 1 | Inferior |
| RAVLT: immediate recall after interference | 23 | Low average |
| RAVLT: delayed recall | 2 | Low average |
| Logical memory: immediate | 5 | Borderline |
| Logical memory: delayed | 22 | Low average |
| Memory of the complex figure of Rey | 15 | Low average |
| Short-term and working memory | | |
| Digit span forwards | 3 | Borderline |
| Digit span backwards | 3 | Borderline |
| Corsi block span forwards | 3 | Borderline |
| Corsi block span backwards | 7 | Low average |
| Visoconstructive skills | | |
| Copy of the complex figure of Rey | 9 | Low average |
| Verbal fluency | | |
| Semantic (animals) | 53 | Average |
| Phonological (F, A, S) | 1 | Inferior |
| Attention – CPT-II | | |
| Omissions errors | 99 | Superior |
| Commissions errors | 99 | Superior |
| Reaction time (RT) mean | 37 | Average |
| Reaction time (RT)_SE | 87 | High average |
| Variability | 99 | Superior |
| Perseverations | 99 | Superior |
| Hit RT block change | 97 | Superior |
| Hit SE block change | 97 | Superior |
| Hit RT ISI block change | 95 | Superior |
| Hit SE RT ISI block change | 91 | High average |
| Inhibition control – five digits test | | |
| Reading task (time) | 45 | Average |
| Counting task (time) | 15 | Low average |
| Choosing task (time) | 45 | Average |
| Shifting task (time) | 5 | Borderline |

canthus, epicanthus, anteverted nostrils, narrow palate, and micrognatia. Camptodactyly of 3rd and 4th fingers of the right hand and 5th finger of the left hand were also observed (Fig. 1c). The patient presented hypothyroidism due to choroid nodular goiter under treatment for 2 years. She was submitted to a neuropsychological assessment in which the Brazilian version of the Wechsler Abbreviated Intelligence Scale-WASI [Trentini et al., 2011] and the Vineland Adaptive Behavioral Scale – VABS-II [Sparrow, 2011] were used to assess intellectual performance. A flexible battery of neuropsychological tests was used for the assessment of specific cognitive functions, prioritizing Brazilian standards whenever available [Lezak et al., 2004]. In addition, the Brazilian versions of the Beck´s Depression [Gomes-Oliveira et al., 2012], and Anxiety [Gorenstein and Andrade, 1996] scales as well as the Adult Self-Report Scale for screening of attention deficit hyperactivity disorder – ADHD [Mattos et al., 2006] were applied. The analysis of the WASI revealed indexes of full intellectual quotient (IQ) in deficiency levels (64); a significantly better performance was observed on the nonverbal domain (performance IQ 75) in comparison to verbal domain (verbal IQ 55). According to the patient's answers on the VABS-II, the main domains of adaptive behavior (communication, daily living skills, socialization, and motor skills) were well developed (standard scores higher than 80). Along the assessment, she showed appropriate basic oral and written communication skills as well as autonomy in the use of public transportation and management of small amounts of money. Results for the neuropsychological tests focusing on cognitive functions are shown in Table 1.

*G-Banding and Molecular Cytogenetic Evaluation*

G-banding was performed on lymphocyte cultures using standard methods, based on the analysis of 40 metaphase cells. Genomic DNA was isolated from peripheral blood using Gentra Puregene Kit (Qiagen-Sciences). Chromosomal microarray was performed using the Affymetrix CytoScan® HD Array (Affymetrix) and was analyzed by the Chromosome Analysis Suite (ChAS) software (Affymetrix), version 3.3, based on GRCh37/hg19.

*Breakpoint Mapping*

The breakpoints of the translocations were mapped by NGS of microdissected and amplified derivative chromosomes as previously described [Jancuskova et al., 2013]. Briefly, amplified DNA fragments were purified using a gel extraction kit (Qiagen) followed by a MinElute PCR purification kit (Qiagen). Afterwards, 454 library preparation, clonal amplification (using the emPCR Lib-L Kit for the GS Junior, Roche), and sequencing were done according to the manufacturer's instructions [Jancuskova et al., 2013]. Bioinformatic analysis was also performed as previously described [Jancuskova et al., 2013]. In summary, sequence reads from the GS Junior runs were analyzed using the Breakpoint Locator software [R. Plachy, unpubl. data], which enables individual reads to be mapped to a reference chromosome sequence (GRCh37/hg19). Parameters including percentage of homology, minimum length to be considered positive, and minimal difference in homology were adjusted to maximize the number of used reads with the minimal possible false-positive matches.

The junction points identified by NGS were validated by Sanger sequencing. Primers (d4-F5: CTTCCTAATTTGCGGGACAA; d4-R5: ACTCACCCCCAAGTTCTGTG; d7-F1: CATTAAGACACTGTTTCCACAGG; d7-R1: CAGACGGGGCAACAAGTAAT) were designed around the breakpoints, and long-range PCR was performed as previously described [Guilherme et al., 2015]. Amplicons were purified and sequenced with the BigDye® Terminator v.3.1 Cycle Sequencing Kit (Applied Biosystems) and an ABI PRISM 3500xl genetic analyzer (Thermo Fisher Scientific).

*Quantitative RT-PCR*

For both genes disrupted at the breakpoints (*PCDH10* and *TNRC18*), expression analysis by reverse transcription quantitative PCR (RT-qPCR) was performed with TaqMan assays (Thermo Fisher Scientific). *GAPDH* and *ACTB* genes were used as internal controls. Eight female individuals (7–51 years) were selected from the healthy population as control individuals for gene expression evaluation. The following Taqman assays were used: Hs00905888 (for *PCDH10* – ENST00000264360.6: exons 1–2, "T1" in Fig. 1e), Hs01396265 (for *TNRC18* – ENST00000430969.5: exons 4–5, "T2" in Fig. 1e), and Hs01396267 (for *TNRC18* – ENST00000430969.5: exons 22–23, "T3" in Fig. 1e). These 2 isoforms (ENST00000264360.6 and ENST00000430969.5) were used as references for *PCDH10* and *TNRC18* transcripts, respectively. cDNA was synthetized using the High Capacity cDNA Reverse Transcription kit (Thermo Fisher Scientific). cDNA samples were assayed in technical triplicate with standard PCR conditions of the 96-Well Fast Thermal Cycling (Thermo Fisher Scientific) and Applied Biosystems 7900HT Sequence Detection System (Thermo Fisher Scientific). A qualitative analysis was performed to assess the relative gene expression between the proband and controls as previously described [Moysés-Oliveira et al., 2019].

## Results

G-banding revealed an apparently balanced translocation between chromosomes 4 and 7 described as 46,XX,t(4;7)(q27;p22)dn (Fig. 1d, e). Chromosomal microarray confirmed that the patient presented a balanced rearrangement. The breakpoints of the translocations were defined by sequencing of microdissected derivative chromosomes and posterior validation by Sanger sequencing (Fig. 1f, g), which revealed the result:

46,XX,t(4;7)(q27;p22)dn,seq[GRCh37] t(4;7)(q28.3;p22.1)

g.[chr4:pter_cen_134113976::chr7:5365447_pter]

g.[chr4:qter_1341139(77–80)::chr7:53654(57–60)_cen_qter]

Sanger sequencing also allowed for the observation of mutational signatures in the breakpoint regions. The breakpoint on chromosome 7 was located at a SINE (short interspersed nuclear elements) repeat element from the Alu family, while the breakpoint on chromosome 4 did not disrupt any repeat element. Thirteen nucleotides were deleted on chromosome 7, and a microhomology of 3 nucleotides was observed on derivative chromosome 7 (Fig. 1g). No insertions, duplications or homologies were observed.

The translocation resulted in the disruption of the *PCDH10* gene in exon 5 at 4q28.3 and disruption of *TNRC18* in intron 19 at 7p22.1. For gene expression study of *TNRC18*, 2 probes were used. One probe, addressed to a region upstream to the breakpoint, showed unmodified expression levels in the patient when compared to controls (controls' $2^{-\Delta\Delta Ct}$ mean = 0.9; controls' $2^{-\Delta\Delta Ct}$ standard deviation = 0.3). The other probe, downstream to the breakpoint, showed approximately 50% reduction of expression in the patient compared to healthy individuals (controls' $2^{-\Delta\Delta Ct}$ mean = 2.3; controls' $2^{-\Delta\Delta Ct}$ standard deviation = 0.4) (Fig. 1h, i). For *PCDH10* (ENST00000264360.6), a probe upstream to the breakpoint was tested, but it did not detect any expression in the patient nor in the controls.

## Discussion

The patient's karyotype and chromosomal microarray revealed a balanced translocation between chromosomes 4q27 and 7p22, indicating that her abnormal phenotype could be caused by gene disruptions at the breakpoints. Sequencing of the breakpoint regions showed disruption of *PCDH10* and *TNRC18*, resulting in chimeric genes. Sanger sequencing of the junction points revealed mutational signatures that were used to infer which mechanisms of formation were most likely to be responsible for the translocation. The deletion of a few nucleotides at the junction points and the presence of microhomology are suggestive of either non-homologous end joining [Gu et

al., 2008] or microhomology-mediated break-induced repair mechanisms [Hastings et al., 2009].

The expression assays for *PCDH10* were inconclusive, because this gene did not show expression in peripheral blood of control individuals. In accordance with our results, *PCDH10* whole blood expression levels in the GTEx database is virtually null (TPM = 0.01) (https://gtexportal.org/home/gene/PCDH10). Regarding the expression of *TNRC18*, the patient presented a variable expression profile depending on the region of the transcript assessed. The exons upstream to the breakpoint (T2 – exon junction 4–5) showed unmodified expression, while the exons downstream to the breakpoint (T3 – exon junction 22–23) were downregulated (Fig. 1h, i). *TNRC18* is subject to extensive alternative splicing and has 8 coding protein isoforms annotated in Ensembl, including one isoform – ENST00000434361.5 – that was not directly disrupted by the translocation's breakpoints and contains the sequence corresponding to junction between exons 4 and 5 but splices out the 3′ region of the transcript starting from exon 6. Thus, the *TNRC18* disruption might have different relative impacts over its isoforms, explaining the divergence found between T2 and T3 expression assays. Alternatively, the unmodified expression levels in the patient shown by T2 assay could indicate a possible formation of a chimeric transcript between *TNRC18* and *PCDH10* in the derivative chromosomes. In der(4), the *TNRC18* downstream segment would be under the control of the *PCDH10* promoter, which is not active in whole blood, leading to the reduced expression level shown by T3. Consistent with this latter hypothesis, *PCDH10* is transcribed from the sense strand, while *TNRC18* is transcribed from the antisense strand. Since this is a p-q translocation, the chimeric genes are in phase for transcription at the junction points (Fig. 1e). Due to the lack of expression of *PCDH10* in peripheral blood, we could not further investigate the formation of putative chimeric transcripts. However, the production of a hybrid mRNA in other tissues and cell types beyond peripheral blood cannot be excluded. Both genes are considered as intolerant to loss of function variations according to gnomAD, with pLI = 0.89 for *PCDH10* and pLI = 0.99 for *TNRC18* [Lek et al., 2016]. Thus, regardless the putative clinical consequence of these possible chimeric transcripts, the phenotype could be related to the loss of function of the disrupted genes. Predicting the functional impact of the novel transcripts' structure on protein expression represents a much more challenging task. The 7p22 breakpoint disrupted *TNRC18* in exon 19 and did not alter the reading frame, leaving the first 2,049 codons intact. However, the *TNRC18* transcript under the *TNRC18* promoter lost its C-terminal portion that codes for the bromo adjacent homology (BAH) domain. Although the role of this domain for TNRC18 function is unclear, this loss might disturb protein interactions, regulation, and chromatin binding activity. The 4q27 breakpoint disrupted *PCDH10* in its 3′-UTR after the stop codon. An alteration of the length of the 3′-UTR can have an important functional impact by disturbing polyadenylation, binding of microRNAs and RNA-binding proteins, thus leading to variations in transcript stability, abundance, translation, and localization [Mariella et al., 2019]. Therefore, even without affecting the *PCHD10* open reading frame, the *PCHD10* 3′-UTR disruption could impair the gene function.

*PCDH10* is highly expressed in brain tissues (https://gtexportal.org/home/gene/PCDH10), is involved in the development and maintenance of the nervous system [Uemura et al., 2007], has been implicated in autism [Morrow et al., 2008; Bucan et al., 2009], and its loss-of-function modeling in mouse recapitulates social interaction impairment [Schoch et al., 2017]. Even though our patient presented a full IQ of 64 and a poor performance especially in the verbal domain of WASI, she did not present a typical case of intellectual disability, since her scores for all adaptive behaviors were within average ranges. It is worth mentioning that many individuals with intelligence scores compatible with intellectual disability classification present well-developed adaptive skills when stimulated from an early age. Scores obtained on the CPT-II, Verbal Fluency test, and Five-Digit (shifting) tests are compatible with a profile of ADHD associated to self-regulation difficulties. Finally, according to the patient's answers in the behavioral scales, it no clinical criteria for any of the neuropsychiatric conditions investigated (anxiety, depression and ADHD) were reached. However, she did not show much engagement in responding to the scales. Therefore, *PCDH10* gene disruption might be related to our patient's neurodevelopmental delay.

The other disrupted gene (*TNRC18*) is still poorly characterized and its function is unknown. Thus, there are no evidences to infer whether its disruption is associated with the patient's clinical features. Although, pathogenic single nucleotide variants in this gene have never been reported in the literature or clinical databases (ClinVar and OMIM), rare variants in *TNRC18* have been recently described in exome aggregation cohorts for neuropsychiatric disorders in preprint manuscripts [Nguyen et al., 2017; Mao et al., 2018]. Even though *TNRC18* is disrupted by the translocation and the expression of the downstream region to the breakpoint was downregulat-

ed, this gene's clinical significance remains unknown. The description of our patient's clinical features has the potential to contribute to the elucidation of the gene function and its potential role in disease. In addition, this work highlights the importance of breakpoint mapping at nucleotide resolution in balanced chromosomal rearrangements in order to better identify the pathogenic mechanisms involved in the phenotype manifestations and improve the genotype-phenotype correlation.


## Acknowledgement

We thank the patients and families and acknowledge Nadezda Kosyakova and Tereza Jancuskova for their technical support.


## Statement of Ethics

A peripheral blood sample was collected after written appropriate informed consent and approval of the local ethics committee (CEP 0028/2015).

## Conflict of Interest Statement

The authors have no conflicts of interest to declare.


## Funding Sources

This work was supported by São Paulo Research Foundation (FAPESP) [grant 2014/11572–8 to MIM] and by the Coordenação de Aperfeiçoamento de Pessoal de Nível Superior-Brasil (CAPES).


## Author Contributions

M.Z., A.D.-B., and M.M.-O. planned, performed the experiments, and wrote the manuscript. C.B.M. performed the neuropsychological evaluation. M.A.P.R. performed the clinical evaluation. T.L. planned, performed the experiments, and revised the manuscript. M.I.M. planned the experiments, wrote and revised the manuscript.

## References


Aristidou C, Koufaris C, Theodosiou A, Bak M, Mehrjouy MM, et al: Accurate breakpoint mapping in apparently balanced translocation families with discordant phenotypes using whole genome mate-pair sequencing. PLoS One 12:e0169935 (2017).

Aristidou C, Theodosiou A, Bak M, Mehrjouy MM, Constantinou E, et al: Position effect, cryptic complexity, and direct gene disruption as disease mechanisms in de novo apparently balanced translocation cases. PLoS One 13:e0205298 (2018).

Bucan M, Abrahams BS, Wang K, Glessner JT, Herman EI, et al: Genome-wide analyses of exonic Copy number variants in a family-based study point to novel autism susceptibility genes. PLoS Genet 5:e1000536 (2009).

Córdova-Fletes C, Domínguez MG, Delint-Ramirez I, Martínez-Rodríguez HG, Rivas-Estilla AM, et al: A de novo t(10;19)(q22.3;q13.33) leads to ZMIZ1/PRR12 reciprocal fusion transcripts in a girl with intellectual disability and neuropsychiatric alterations. Neurogenetics 16:287–298 (2015).

Funderburk SJ, Spence MA, Sparkes RS: Mental retardation associated with "balanced" chromosome rearrangements. Am J Hum Genet 29:136–141 (1977).

Gomes-Oliveira MH, Gorenstein C, Lotufo Neto F, Andrade LH, Wang YP: Validation of the Brazilian Portuguese version of the Beck Depression Inventory-II in a community sample. Rev Bras Psiquiatr 34:389–394 (2012).

Gorenstein C, Andrade L: Validation of a Portuguese version of the Beck Depression Inventory and the State-Trait Anxiety Inventory in Brazilian subjects. Brazilian J Med Biol Res 29:453–457 (1996).

Di Gregorio E, Bianchi FT, Schiavi A, Chiotto AMA, Rolando M, et al: A de novo X;8 translocation creates a *PTK2-THOC2* gene fusion with THOC2 expression knockdown in a patient with psychomotor retardation and congenital cerebellar hypoplasia. J Med Genet 50:543–551 (2013).

Gu W, Zhang F, Lupski JR: Mechanisms for human genomic rearrangements. Pathogenetics 1:4 (2008).

Guilherme RS, Hermetz KE, Varela PT, Perez ABA, Meloni VA, et al: Terminal 18q deletions are stabilized by neotelomeres. Mol Cytogenet 8:32 (2015).

Hastings PJ, Ira G, Lupski JR: A microhomology-mediated break-induced replication model for the origin of human copy number variation. PLoS Genet 5:e1000327 (2009).

Jancuskova T, Plachy R, Stika J, Zemankova L, Hardekopf DW, et al: A method to identify new molecular markers for assessing minimal residual disease in acute leukemia patients. Leuk Res 37:1363–1373 (2013).

Lek M, Karczewski KJ, Minikel EV, Samocha KE, Banks E, et al: Analysis of protein-coding genetic variation in 60,706 humans. Nature 536:285–291 (2016).

Lezak MD, Howieson DB, Loring DW: Neuropsychological Assessment, ed 4 (Oxford Univ Press, New York 2004).

Liang D, Wang Y, Ji X, Hu H, Zhang J, et al: Clinical application of whole-genome low-coverage next-generation sequencing to detect and characterize balanced chromosomal translocations. Clin Genet 91:605–610 (2017).

Mao F, Wang L, Zhao X, Xiao L, Li X, et al: De novo mutations involved in post-transcriptional dysregulation contribute to six neuropsychiatric disorders. bioRxiv:175844 (2018).

Mariella E, Marotta F, Grassi E, Gilotto S, Provero P: The length of the expressed 3′ UTR is an intermediate molecular phenotype linking genetic variants to complex diseases. Front Genet 10:714 (2019).

Mattos P, Segenreich D, Saboya E, Louzã M, Dias G, Romano M: Adaptação transcultural para o português da escala Adult Self-Report Scale para avaliação do transtorno de déficit de atenção/hiperatividade (TDAH) em adultos. Arch Clin Psychiatry (São Paulo) 33:188–194 (2006).

Menten B, Maas N, Thienpont B, Buysse K, Vandesompele J, et al: Emerging patterns of cryptic chromosomal imbalance in patients with idiopathic mental retardation and multiple congenital anomalies: a new series of 140 patients and review of published reports. J Med Genet 43:625–633 (2006).

Morrow AM, Yoo S-Y, Flavell SW, Kim T-K, Lin Y, et al: Identifying autism loci and genes by tracing recent shared ancestry. Science 321: 218–223 (2008).

Moysés-Oliveira M, Di-Battista A, Zamariolli M, Meloni VA, Bragagnolo S, et al: Breakpoint mapping at nucleotide resolution in X-autosome balanced translocations associated with clinical phenotypes. Eur J Hum Genet 27: 760–771 (2019).

Nguyen HT, Bryois J, Kim A, Dobbyn A, Huckins LM, et al: Integrated Bayesian analysis of rare exonic variants to identify risk genes for schizophrenia and neurodevelopmental disorders. bioRxiv:135293 (2017).

Nilsson D, Pettersson M, Gustavsson P, Förster A, Hofmeister W, et al: Whole-genome sequencing of cytogenetically balanced chromosome translocations identifies potentially pathological gene disruptions and highlights the importance of microhomology in the mechanism of formation. Hum Mutat 38:180–192 (2017).

Ravel C, Berthaut I, Bresson JL, Siffroi JP, Genetics Commission of the French Federation of CECOS, Stiffroi JP: Prevalence of chromosomal abnormalities in phenotypically normal and fertile adult males: large-scale survey of over 10,000 sperm donor karyotypes. Hum Reprod 21:1484–1489 (2006).

Redin C, Brand H, Collins RL, Kammin T, Mitchell E, et al: The genomic landscape of balanced cytogenetic abnormalities associated with human congenital anomalies. Nat Genet 49:36–45 (2017).

Schluth-Bolard C, Diguet F, Chatron N, Rollat-Farnier P-A, Bardel C, et al: Whole genome paired-end sequencing elucidates functional and phenotypic consequences of balanced chromosomal rearrangement in patients with developmental disorders. J Med Genet 56: 526–535 (2019).

Schneider A, Puechberty J, Ng BL, Coubes C, Gatinois V, et al: Identification of disrupted *AUTS2* and *EPHA6* genes by array painting in a patient carrying a de novo balanced translocation t(3;7) with intellectual disability and neurodevelopment disorder. Am J Med Genet A 167A:3031–3037 (2015).

Schoch H, Kreibich AS, Ferri SL, White RS, Bohorquez D, et al: Sociability deficits and altered amygdala circuits in mice lacking Pcdh10, an autism associated gene. Biol Psychiatry 81:193–202 (2017).

Sparrow SS: Vineland Adaptive Behavior Scales, in Encyclopedia of Clinical Neuropsychology, pp 2618–2621 (Springer, New York 2011).

Trentini C, Yates D, Heck V: The adaptation, reliability, validity and standardization of the Wechsler abbreviated scale of intelligence to the Brazilian reality. Int Test Comm Newsl 26: 7–9 (2011).

Uemura M, Nakao S, Suzuki ST, Takeichi M, Hirano S: OL-Protocadherin is essential for growth of striatal axons and thalamocortical projections. Nat Neurosci 10:1151–1159 (2007).

Warburton D: De novo balanced chromosome rearrangements and extra marker chromosomes identified at prenatal diagnosis: clinical significance and distribution of breakpoints. Am J Hum Genet 49:995–1013 (1991).

Zepeda-Mendoza CJ, Menon S, Morton CC: Computational prediction of position effects of human chromosome rearrangements. Curr Protoc Hum Genet 97:e57 (2018).